

Keck Diffraction-Limited Imaging of the Young Quadruple Star System HD 98800¹

L. Prato² and A. M. Ghez³

Department of Physics and Astronomy, UCLA, Los Angeles, CA 90095-1562

R. K. Piña, C. M. Telesco, and R. S. Fisher

Department of Astronomy, University of Florida, Gainesville, FL 32611

P. Wizinowich, O. Lai, D. S. Acton, and P. Stomski

W. M. Keck Observatory, 65-1120 Mamalahoa Hwy, Kamuela, HI 96743

ABSTRACT

This paper presents diffraction-limited 1–18 μm images of the young quadruple star system HD 98800 obtained with the W. M. Keck 10-m telescopes using speckle and adaptive optics imaging at near-infrared wavelengths and direct imaging at mid-infrared wavelengths. The two components of the visual binary, A and B, both themselves spectroscopic binaries, were separable at all wavelengths, allowing us to determine their stellar and circumstellar properties. Combining these observations with spectroscopic data from the literature, we derive an age of $\sim 10^7$ years, masses of 0.93 and 0.64 M_{\odot} and an inclination angle of 58° for the spectroscopic components of HD 98800 B, and an age of $\sim 10^7$ years and a mass of 1.1 M_{\odot} for HD 98800 Aa. Our data confirm that the large mid-infrared excess is entirely associated with HD 98800 B. This excess exhibits a black body temperature of 150 K and a strong 10 μm silicate emission feature. The theoretical equilibrium radius of large, perfectly absorbing, 150 K grains around HD 98800 B is 2.4 AU, suggesting a circum-spectroscopic binary distribution. Our observations set important upper limits on the size of the inner dust radius of ~ 2 AU (from the mid-infrared data) and on the quantity of scattered light of $< 10\%$ (from the H-band data). For an inner radius of 2 AU, the dust distribution must have a height of at least 1 AU to account for the fractional dust luminosity of $\sim 20\% L_B$. Based on the scattered light limit, the dust grains responsible for the excess emission must have an albedo of < 0.33 . The presence of the prominent silicate emission feature at 10 μm implies dust grain radii of $\gtrsim 2\mu\text{m}$. The total mass of the dust, located in a circumbinary disk around the HD 98800 B, is $> 0.002 M_{\oplus}$. The orbital dynamics of the A–B pair are probably responsible for the unusual disk geometry.

¹To appear in the *Astrophysical Journal*

²lprato@astro.ucla.edu

³Packard Fellow

Subject headings: binaries: visual, spectroscopic — circumstellar matter — infrared: stars — stars: individual (HD 98800) — stars: pre–main-sequence

1. Introduction

HD 98800 is one of the most frequently studied members of the TW Hydra Association because of its notably large fractional infrared (IR) luminosity excess, first detected by the IRAS satellite (Walker and Wolstencroft 1988; Zuckerman and Becklin 1993). Hipparcos results reported by Favata et al. (1998) indicate that HD 98800 is at a distance of 47.6 pc, which has led to recent age estimates for this K5 system of ~ 7 Myr, suggesting that the stars are pre–main-sequence (PMS) (Fekel and Bopp 1993; Soderblom et al. 1996; Webb et al. 1999; Jensen, Cohen, and Neuhäuser 1998). The lack of obvious signatures of active accretion, such as hydrogen emission lines (Soderblom et al. 1996; Webb et al. 1999) and near-IR excess (e.g. Low, Hines, and Schneider 1999), implies that the observed mid-IR excess probably originates in a dusty disk with a central gap.

Complicating both the dynamics and the analysis of the HD 98800 system is its multiplicity. Innes (1909) identified it as a visual binary; its current north-south angular separation of $0.''8$ corresponds to a projected linear separation of 38 AU. Orbital solutions for the visual binary are not unique because only linear motion has been observed during the last nine decades. Torres et al. (1995) initially found a family of orbits with extremely high eccentricity (~ 0.9), e , and periods, P , $> 10^5$ years. Using the Hipparcos data, and with knowledge of the PMS nature of the system, Tokovinin (1999) published a different set of orbital solutions with moderate 300–430 year periods and 0.3–0.6 eccentricities. Tokovinin’s orbits are probably more reliable since they incorporate better values for the component masses and the Hipparcos distance, thus improving the determination of e and P (Torres 2000). Spectroscopic measurements have shown that each component of the visual binary has a companion. The southern component, HD 98800 A, is a single-lined spectroscopic binary (SB) with $P=262$ days and $e=0.484$, while the northern component, HD 98800 B, is a double-lined SB with $P=315$ days and $e=0.781$ (Torres et al. 1995). The presence of numerous components raises questions regarding the relationship between the stars and the dust: Where does the dust reside? Is the interaction between the multiple stellar components and the dust responsible for HD 98800’s unusually large fractional IR excess? And more speculatively, can planets form and survive within this system?

To address these questions, we carried out a 1– $18\mu\text{m}$ diffraction-limited imaging study with the W. M. Keck 10-m telescopes, complementing results presented in several recent papers. Soderblom et al. (1998) and Low et al. (1999) used, respectively, the WFPC2 and NICMOS cameras on the *Hubble Space Telescope* to characterize the stellar parameters of the individual A and B components and to search for scattered light from the dust. Gehrz et al. (1999) used the ESO 3.6-m telescope to study the system at $4.7\mu\text{m}$ and $9.7\mu\text{m}$, locating the bulk of the dust around the B component. Koerner et al. (2000) combined mid-IR with published millimeter wavelength data, dramatically

illustrating that the excess emission is associated with HD 98800 B and modelling the dust distribution. With a factor of 2–4 times higher spatial resolution than most previous observations, the measurements in this study are used to characterize the physical properties and spatial distribution of the dust and stars in HD 98800 and to construct a paradigm for the system. The observations are described in §2 and the analysis and results in §3. A discussion is provided in §4 and a summary in §5.

2. Observations

2.1. Mid-Infrared Camera Observations

HD 98800 (HIP 55505) and the photometric standard μ UMa were observed at the Keck II 10-m telescope on 1998 May 11 (UT) using OSCIR, the University of Florida mid-infrared camera. The camera has a Rockwell 128×128 Si:As Blocked Impurity Band (BIB) array with a plate scale of 0."062/pixel on Keck II, yielding a 7."9×7."9 field of view. The observations were made through light cirrus clouds in four broad-band filters, K (2.2 μ m), M (3.5 μ m), N (10.8 μ m) and IHW18 (18.2 μ m), and six narrow-band filters ($\Delta\lambda \sim 1\mu$ m), 7.9 μ m, 8.8 μ m, 9.8 μ m, 10.3 μ m, 11.7 μ m and 12.5 μ m. An 8" off-source throw in the north-south direction generated a standard chop-nod pattern. Exposures of 30 ms were coadded to produce images at each chop and nod position. The chop frequency was 4.1 Hz and the nod time was approximately 30 seconds. On-source integration times were approximately 45 s for all ten filters. Each nod set was double-differenced to produce background subtracted images. These differenced images were magnified by a factor of 4, registered and summed.

2.2. Near-Infrared Speckle Imaging Observations

Speckle observations of HD 98800 were carried out at the Keck I telescope on 1996 January 4–6 (UT) using the facility 256 x 256 Near-Infrared Camera (NIRC; Matthews and Soifer 1994; Matthews et al. 1996), which has a plate scale of 0."0203/pixel in its high angular resolution mode. Approximately 1,000 short exposures (0.1s) were obtained for HD 98800 and a nearby SAO star through three filters: J ($\lambda_o = 1.25\mu$ m), H ($\lambda_o = 1.65\mu$ m) and K_{cont} ($\lambda_o = 2.2\mu$ m). Each snapshot was individually sky-subtracted, divided by a flat field, and corrected for bad pixels, and then combined with the others at the same wavelength to construct a diffraction-limited image through standard speckle image analysis procedures described in detail elsewhere (e.g., Ghez, Neugebauer, and Matthews 1993).

2.3. Near-Infrared Adaptive Optics Observations

On 1999 May 26 (UT), HD 98000 and a nearby point source, SAO 180158, were observed on Keck II using the natural guide star adaptive optics system and KCAM, a 256x256 NICMOS 3 array with a plate scale of $0.''017/\text{pixel}$ (Wizinowich et al. 2000a,b). HD 98800 proved to be an excellent adaptive optics guide star, in spite of its multiple components, and resulted in observations with Strehl ratios of up to ~ 0.6 for 5s integrations. A total of 20 H-band images were obtained, interleaved with observations of SAO 180158, at different positions on the array. To create the highest quality final map, each image was magnified by a factor of two and the 13 frames with the largest Strehl ratios were combined.

3. Data Analysis and Results

3.1. The Images

Figures 1–3 show the final diffraction-limited images of HD 98800. The resolution ranges from $0.''03$ at $1.25\mu\text{m}$ to $0.''46$ at $18.2\mu\text{m}$. The components of the $0.''8$ north-south pair are easily distinguished out to $12.5\mu\text{m}$. At $18\mu\text{m}$, the southern component, A, is marginally detected at $\sim 3\sigma$. As originally suggested by Gehrz et al. (1999) and confirmed by Koerner et al. (2000) on the basis of their mid-IR data, the dust is associated with the northern component, HD 98800 B. Between $1\text{--}18\mu\text{m}$ there is no evidence of dust around HD 98800 A. Our mid-IR fluxes agree with those of Koerner et al. (2000) to within 1σ at almost every wavelength common to both data sets.

We inspected each component of the wide $0.''8$ pair for spatially resolved structure arising from mid-IR thermal dust emission, near-IR scattered light from the dust, or near-IR photospheric emission from the SB components. Figure 4 is a comparison of the HD 98800 A and B azimuthal averages at mid-IR wavelengths. Since HD 98800 A appeared with HD 98800 B simultaneously in the images at each wavelength, and since no excess emission was evident in its spectral energy distribution (SED) (see §3.2), HD 98800 A is an ideal point source for comparison. At every mid-IR wavelength where the signal to noise ratio is large enough for a meaningful comparison of the data, 8.8, 9.8, 10.3 and $11.7\mu\text{m}$, the HD 98800 B FWHM is comparable to that of HD 98800 A (Figure 4). This suggests that HD 98800 B is unresolved. To avoid averaging over structure that is extended in one particular direction, as might be expected for an inclined disk, one dimensional profiles at position angles of 0° , 45° , 90° and 135° were compared; no position angle dependence was detected. Although the excess emission is unresolved, it is possible to set upper limits on the extent of the dust. A model for HD 98800 B is created from a delta function and a gaussian, representing, respectively, the stellar photospheric contribution and the dust component, where the ratio between the dust and the photosphere is determined from the SED (see Table 1, §3.2.1, and Figure 6). The result is convolved with the PSF (HD 98800 A) and the azimuthally averaged profile compared to that of HD 98800 B. We assign a 3σ upper limit to the radius of the dust

distribution by identifying the broadest gaussian that produces a $\Delta\chi^2 = 3$. At each of the four mid-IR wavelengths analyzed, this upper limit, given in Table 1, is close to ~ 2 AU.

In the J, H, and K-bands, the spatial resolution is ~ 4 – 10 times higher than at $10\mu\text{m}$. By comparing the azimuthally averaged AO H-band profiles of HD 98800 A and B and a point source, Figure 5, it is possible to set a 1σ upper limit of $<10\%$ on the reflected light from the dust around the B component out to a radius of 10 AU. Given this result and the dust fractional luminosity of $0.2L_B$ (Zuckerman and Becklin 1993), we estimate that the grain albedo is less than 0.33. There is no evidence that the HD 98800 A and B subcomponents are resolved (Figures 2 and 3). Combining the orbital elements provided by Torres et al. (1995) and our estimate of 58° for the inclination of the HD 98800 B system (see §3.2.2) to calculate the Ba–Bb separation yields ~ 0.9 AU, or $0.''019$, at the time of our J, H, and K speckle observations.

3.2. Spectral Energy Distributions

3.2.1. Construction of SEDs

Photometry with aperture radii equal to the diffraction limit provided flux ratios for HD 98800 A and B in the mid-IR and near-IR AO images. The flux ratios for the speckle imaging data sets were obtained from visibility fitting (e.g. Ghez et al. 1993). Column 7 of Table 2 lists the results. Absolute photometry from our data sets was compromised by non-photometric conditions. Therefore, the unresolved measurements of Zuckerman and Becklin (1993) provided total flux densities (column 6 of Table 1). These values were combined with the flux ratios to produce the flux densities of the individual components, which, together with other recent measurements, are listed in columns 8 and 9 of Table 2. SEDs for HD 98800 A and B are plotted in Figure 6.

3.2.2. Stellar Properties

The stellar and circumstellar properties of the HD 98800 system are derived from the SEDs. Using the $0.43 - 4.8\mu\text{m}$ flux density measurements, we characterize the photospheric emission with both black body distributions and Kurucz models obtained with the HST Synphot package (Kurucz 1993), using $\log(g)=5$ and solar metallicity (see Soderblom et al. 1998). Table 3 lists the resulting temperatures and luminosities for both models. The two approaches yield comparable quality fits, although, as expected, they differ significantly in terms of implied temperatures. The Kurucz model temperatures agree with those determined spectroscopically by Soderblom et al. (1998) to within 1σ . We therefore preferentially use the Kurucz temperatures, 4500 K for HD 98800 A and 4000 K for HD 98800 B, in our analysis and discussion.

Estimates of the masses and ages for the stellar components are obtained by comparing their luminosities and temperatures to PMS evolutionary models. For the single-lined spectroscopic

binary HD 98800 A, we consider only Aa, using our derived Kurucz model temperature and luminosity. For the double-lined spectroscopic binary HD 98800 B, the luminosity estimate for HD 98800 A, $0.63L_{\odot}$, derived from the Kurucz model (Table 3), is multiplied by the luminosity ratios given by Torres et al. (1995), $L_{Ba}/L_A = 0.5$ and $L_{Bb}/L_A = 0.3$, to identify the Ba and Bb component luminosities. The individual temperatures for HD 98800 Ba and Bb, from Soderblom et al. (1998), case B, are 4250 K and 3700 K, respectively. With these values for the temperatures and luminosities, Figure 7 shows the Aa, Ba and Bb components on the PMS evolutionary tracks of Baraffe et al. (1998), with a mixing length of $\alpha = 1.9$, which the recent results of White et al. (1999) suggest are the most reliable. These tracks yield $M_{Aa} = 1.1 \pm 0.1 M_{\odot}$, $M_{Ba} = 0.93 \pm 0.08 M_{\odot}$ and $M_{Bb} = 0.64 \pm 0.10 M_{\odot}$, with an age of approximately 10^7 years for all components (Table 3).

Our mass estimates for HD 98800 Ba and Bb, together with the mass ratio and the mass functions from Torres et al. (1995), allow us to estimate the inclination angle, i , of the spectroscopic binary. The approach is illustrated in Figure 8, which shows component mass *versus* the inclination angle. The horizontal bands depict the 1σ range for the masses, obtained from the Baraffe et al. (1998) evolutionary tracks, and the curves represent the dynamically determined $M_1 \sin^3 i$ and $M_2 \sin^3 i$. Together these measurements constrain the HD 98800 Ba–Bb inclination angle to be $57.9^{\circ} \pm 0.8$. This procedure was repeated with the tracks of Swenson et al. (1994), D’Antona and Mazzitelli (1994) and D’Antona and Mazzitelli (1997) and values for the inclination of 56.8° , 63.5° and 63.6° , respectively, were obtained. The standard deviation of the mean for the four values of inclination calculated from the different tracks is only 1.8° . Therefore, our estimate of $i_{Ba-Bb} \sim 58^{\circ}$ is robust.

3.2.3. Circumstellar Properties

Figure 9 shows the excess emission, isolated by subtracting the Kurucz model photosphere from the HD 98800 B SED. The $7.9\mu\text{m}$ and $12.5\text{--}100\mu\text{m}$ flux densities are used to fit a black body to the excess, excluding the prominent silicate emission feature at $10\mu\text{m}$. A black body of temperature 150 ± 5 K and luminosity $0.11 \pm 0.02 L_{\odot}$ gives the best fit. Table 4 provides a summary of all the derived dust properties. The IRAS and millimeter wavelength data, which do not resolve HD 98800 A and B, are probably entirely attributable to HD 98800 B, since in our spatially resolved observations the excess between 7.9 and $18.2\mu\text{m}$ is associated solely with the B component. In our discussion we will assume that this is the case.

3.2.4. Grain Properties

As indicated by Skinner, Barlow, and Justtanont (1992) (see their Figure 2) and Sylvester and Skinner (1996), the emission from the HD 98800 B dust is consistent with the presence of large grains, on the order of tens to hundreds of microns in diameter to account for the observed ratio

of infrared to millimeter flux. With the assumption that the dust is optically thin, we estimate a lower limit on the size of gravitationally bound grains stable against blow-out of $r_g > 0.2\mu\text{m}$, deduced from equating the gravitational and radiation pressure forces, given a typical ice grain density of $\sim 1\text{ gm/cm}^3$ (Backman and Paresce 1993). Similarly, for silicate grains, clearly present around HD 98800 B (Figure 9), $\rho \sim 3\text{ gm/cm}^3$, and $r_g > 0.07\mu\text{m}$. However, for silicate grains to emit efficiently at mid-IR wavelengths, i.e. $2\pi r_g/\lambda \lesssim 1$, where $\lambda = 10\mu\text{m}$, they must have $r_g < 1.6\mu\text{m}$ (see <http://www.astro.princeton.edu/~draine/dust/dust.diel.html>). The Poynting-Robertson lifetime of a $\rho = 3\text{ gm/cm}^3$, $r = 1.6\mu\text{m}$ grain is about 23,000 years. Zuckerman and Becklin (1993) calculate a Poynting-Robertson lifetime about five times longer than this based on typically larger grain sizes. Assuming that the dust around HD 98800 B formed at the same time as the stars, which are estimated to be $\sim 10^7$ years old, the relatively short lifetime we calculate requires some mechanism, such as collisions between larger bodies, to resupply the small grain population, as has been pointed out by other authors (e.g., Backman and Paresce 1993). We estimate a lower bound for the total dust mass of $\sim 0.002 M_\oplus$, given a mass absorption coefficient of $\sim 1000\text{ cm}^2/\text{gm}$ and the solid angle for an annulus of inner radius 2 AU and outer radius 5 AU (see §3.1 and §4.1).

4. Discussion

4.1. Disk Structure

The results presented in §3 and in the literature constrain the structure of the disk around HD 98800 B. Our estimates for the albedo, < 0.33 , dust temperature, 150 K, and the total stellar luminosity, $0.58L_\odot$, allow us to calculate the theoretical equilibrium radius of the dust. Because the luminosity comes from two sources, the stars in the highly eccentric spectroscopic binary, we make the simplifying assumption here that the two are equally bright. A numerical solution for the time averaged stellar luminosity as seen from a disk gives a dust equilibrium radius of ~ 2.4 AU from the center of mass of the system.

The criterion of Artymowicz and Lubow (1994), $[(1/2)a(1+e)]+a$, one half the apastron separation of the stars plus the semi-major axis, a , can be used to determine the inner radius of a stable, tidally truncated circumbinary disk. Combining the data given by Torres et al. (1995) for $a_1\sin i$, $a_2\sin i$ and the eccentricity, e , with our estimate of $i = 58^\circ$, yields $a = 1.07$ AU; for a stable disk, the inner radius must therefore be $\gtrsim 2$ AU. The data presented in Table 1 indicate that the 3σ upper observational limit on the inner radius is between 1.8 and 2.1 AU (§3.1), barely consistent with this result.

From the slight photometric variability of the HD 98800 system seen in the Hipparchos data (Soderblom et al. 1998), Tokovinin (1999) infers that the Ba–Bb binary is seen at an inclination of $\sim 90^\circ$ through the circumbinary dust. Given the 10^7 year age of HD 98800 B, and the 315 day orbital period of Ba–Bb, the dust distribution and the stellar orbit are probably coplanar (Lubow 2000). Thus, the 58° inclination angle derived for the spectroscopic binary also applies to the dust.

The large fractional luminosity, $0.2L_B$, requires that the dust be vertically extended, since, at a radius of 2 AU, a thin disk intercepts far too little starlight to account for the dust brightness. A disk of perfectly absorbing grains would have to have a height of at least 1 AU in order to account for the large fractional luminosity if all the light reradiated by the disk were intercepted by the grains at a radius of ~ 2 AU. Given the upper bound on the albedo, 0.33, the height of the disk must be between 1 and 1.5 AU. For a spherical distribution of dust, we expect the fractional luminosity to be greater than the $0.2L_B$ observed; thus, a thick disk geometry is most likely.

The dust around the HD 98800 B spectroscopic binary is located in a circumbinary disk with an equilibrium radius of 2.4 AU, an inner gap of ~ 2 AU, and a vertical extent of >1 AU. To account for the observed $8.8\mu\text{m}$ excess flux density of 0.61 Jy, the outer radius of a disk at 47.6 pc with a 2 AU inner gap and $T=150$ K must be ~ 5 AU if the origin of the emission is primarily black body. (The value listed in Table 2 for the $8.8\mu\text{m}$ flux density includes the stellar photosphere; Figure 6 shows that the dust to photosphere brightness ratio is 2.1 at $8.8\mu\text{m}$.) Cooler dust probably extends further out than 5 AU (Koerner et al. 2000), however, it will eventually be truncated by the dynamical action of the visual binary’s orbit at about one third of the periastron distance between HD 98800 A and B, i.e. at least $\sim 10\text{--}15$ AU, depending on projection effects.

4.2. A Paradigm for the HD 98800 System

We believe that the orbit of the visual binary, HD 98800 A–B, is responsible for the current configuration of the system, since the inclination of this wide pair is $87^\circ\text{--}89^\circ$ (Torres et al. 1995; Tokovinin 1999), while the inclination of HD 98800 Ba–Bb and the associated dust disk is $\sim 58^\circ$. The A–B and the Ba–Bb orbits, and therefore the A–B orbit and the B-component dust disk, are not coplanar. Tidal forces not only may have ripped away circumbinary material from HD 98800 A in the past, but also may perturb the HD 98800 B circumbinary disk in the present, maintaining the small grain population against Poynting-Robertson drag and giving rise to its unusual vertical extension. Disk warping as a result of binary perturbations from a non-coplanar companion has been described by Terquem and Bertout (1996) and Larwood et al. (1996). These perturbations could cause precession of the HD 98800 B dust orbital plane, maintaining the 58° inclination constant but varying the orientation of the disk. Such changes would cause the disk to be at times perpendicular and at times parallel to the A–B orbital plane. We speculate that similar dynamics destroyed the disk around HD 98800 A, anomalous in that no evidence of dust is apparent, and currently maintain the configuration of the HD 98800 B dust, still prominent although the stellar ages are about 400 times greater than the Poynting-Robertson lifetime of the grains, and apparently significantly vertically extended. Orbital periods in the models proposed by Tokovinin (1999) range from 300 to 430 years, allowing for relatively short term periodic perturbations of the HD 98800 B disk, initiated during periastron passage with HD 98800 A.

5. Summary

We have resolved the $0.''8$ visual binary components in the young stellar system HD 98800 from $1\text{--}18\mu\text{m}$, obtaining complete resolved observations of the silicate emission feature at $10\mu\text{m}$ through six narrow-band filters, and of the $18.2\mu\text{m}$ flux. The mid-IR excess appears to be azimuthally symmetric and is entirely associated with HD 98800 B, a double-lined spectroscopic binary. The PSF of HD 98800 B is similar to that of HD 98800 A in at least the 4 filters spanning $8.8\text{--}11.7\mu\text{m}$, and implies an upper limit for the mid-IR emission of ~ 2 AU. There is no evidence for any excess emission from HD 98800 B at near-IR wavelengths, from $1.2\text{--}4.8\mu\text{m}$. Our H-band AO images yield an upper bound on the reflected light from the HD 98800 B excess of $<10\%$ and therefore an albedo for the grains of <0.33 .

On the PMS tracks of Baraffe et al. (1998) the observable components of HD 98800 appear coeval with an age of $\sim 10^7$ years. Our calculations of the stellar parameters allow us to estimate new masses for HD 98800 Aa, Ba and Bb of 1.1, 0.93 and $0.64 M_{\odot}$, respectively. From the masses of the Ba–Bb pair we derive $i = 58^{\circ}$ and, in turn, a semi-major axis of 1.07 AU. For the wide visual binary pair, $i = 90$ (Torres et al. 1995; Tokovinin 1999); thus, the orbits of A–B and Ba–Bb are not coplanar. A black body fit to the SED of the HD 98800 B mid-IR excess indicates a dust temperature of 150 K. If optically thin, the radii of the grains span a range from $\sim 2\mu\text{m}$ through hundreds, possibly thousands, of microns. The total mass of the dust is $>0.002 M_{\oplus}$. The Poynting-Robertson lifetime of the smallest grains is $\sim 23,000$ years, suggesting that the disk requires replenishment.

Based on both observational and dynamical considerations, the inner radius of the dust around HD 98800 B is ~ 2 AU. Thus, it must be a circum-spectroscopic binary structure. The outer radius must be at least ~ 5 AU to account for the observed flux densities, and cool dust may extend out as far as $\gtrsim 10$ AU, where it is eventually tidally truncated by the orbit of HD 98800 A. Given the high fractional luminosity, the vertical extent of the dust must be ~ 1.5 AU. Thus, the HD 98800 B spectroscopic binary is surrounded by a thick dust disk, probably in the same orbital plane as the central binary, whereas around HD 98800 A, no evidence for any dust has been detected. We speculate that, since the orbits of the A–B pair and the dust disk are not coplanar, dynamical interactions at the A–B orbit periastron are responsible for the survival against Poynting-Robertson drag and the vertical structure of the B component disk, as well as for the dissipation of the A component disk. Precession of the orientation of the dust plane resulting from perturbations driven by HD 98800 A may have allowed various dynamical processes to take place at different times. It seems unlikely that planetary formation would flourish in such an environment.

We thank the staff and in particular the Observing Assistants, Joel Aycock and Chuck Sorenson, of the W. M. Keck Observatory for their logistic and technical support. We are grateful to Peter Bodenheimer, Mike Jura, Steve Lubow, Mike Simon, Alycia Weinberger, Mark Wyatt, and Ben Zuckerman for helpful discussions and suggestions and to Russel White for producing Figure 7. We thank Bruce Draine and an anonymous referee for useful comments on the manuscript. The data presented here were obtained at the W. M. Keck Observatory, operated as a scientific partnership between the California Institute of Technology, the University of California, and the National Aeronautics and Space Administration (NASA). The Observatory was made possible by the contributions of the W. M. Keck Foundation. This research was supported by the NASA Origins of Solar Systems Program grant NAG5-6975 and the Packard Foundation; additional funding for the AO portion of this work was provided by the NSF Science and Technology Center for Adaptive Optics.

REFERENCES

- Artymowicz, P., and Lubow, S. 1994, *ApJ*, 421, 651
- Backman, D. E., and Paresce, F. 1993, in *Protostars and Planets III*, ed. E. H. Levy and J. I. Lunine (Tucson: Univ. of AZ Press), 1253
- Baraffe, I., Chabrier, G., Allard, F., and Hauschildt, P. H. 1998, *A&A*, 337, 403
- D’Antona, F., and Mazzitelli, I. 1994, *ApJS*, 90, 467
- D’Antona, F., and Mazzitelli, I. 1997, ‘Evolution of Low Mass Stars’ in *“Cool Stars in Clusters and Associations”*, eds. G. Micela and R. Pallavicini, *Mem. S. A. It.*, 68, 807
- Favata, F., Micela, G., Sciortino, S., and D’Antona, F. 1998, *A&A*, 335, 218
- Fekel, F. C., and Bopp, B. W. 1993, *ApJ*, 49, L89
- Gehrz, R. D., Smith, M., Low, F. J., Kratter, J., Nollenberg, J. G., and Jones, T. J. 1999, *ApJ*, 512, L55
- Ghez, A. M., Neugebauer, G., and Matthews, K. 1993, *AJ*, 106, 2005
- Innes, R. T. A. 1909, *Transvaal Obs. Circ.*, 1, 1
- Jensen, E. L. N., Cohen, D. H., and Neuhäuser, R. 1998, *ApJ*, 116, 414
- Koerner, D. W., Jensen, E. L. N., Cruz, K., Guild, T. B., and Gultekin, K. 2000, *ApJ*, 533, L37
- Kurucz, R. L. 1993, SYNTHE spectrum synthesis programs and line data, Kurucz CD-ROM, Cambridge, MA: Smithsonian Astrophysical Observatory

- Larwood, J. D., Nelson, R. P., Papaloizou, J. C. B., and Terquem, C. 1996 MNRAS, 282, 597
- Low, F. J., Hines, D. C., and Schneider, G. 1999, ApJ, 520, L45
- Lubow, S. 2000, private communication
- Matthews, K., Ghez, A. M., Weinberger, A. J., and Neugebauer, G. 1996, PASP, 108, 615
- Matthews, K., and Soifer, B. T. 1994, *Astronomy with Infrared Arrays: The Next Generation*, ed. I. McLean, Kluwer Academic Publications (Astrophysics and Space Science, v. 190, p. 239)
- Palla, F., and Stahler, S. W. 1999, ApJ, 525, 772
- Rucinski, S. 1993, IAUC, 5788
- Skinner, C. J., Barlow, M. J., and Justtanont, K. 1992, MNRAS, 255, 31
- Soderblom, D. R., Henry, T. J., Shetrone, M. D., Jones, B. F., and Saar, S. H. 1996, ApJ, 460, 984
- Soderblom, D. R., et al. 1998, ApJ, 498, 385
- Stern, S. A., Weintraub, D. A., and Festou, M. C. 1993, IAUC, 6003
- Swenson, J. H., Faulkner, J., Rogers, F. J., and Iglesias, C. A. 1994, ApJ, 425, 286
- Sylvester, R. J., and Skinner, C. J. 1996, MNRAS, 283, 457
- Sylvester, R. J., Skinner, C. J., Barlow, M. J., and Mannings, V. 1996, MNRAS, 279, 915
- Terquem, C., and Bertout, C. 1996, MNRAS, 279, 415
- Tokovinin, A. A. 1999, AstL, 25, 669
- Torres, G. 2000, private communication
- Torres, G., Stefanik, R. P., Latham, D. W., and Mazeh, T. 1995, ApJ, 452, 870
- Walker, H., and Wolstencroft, R. D., PASP, 100, 1509
- Webb, R. A., Zuckerman, B., Platais, I., Patience, J., White, R. J., Schwartz, M. J., and McCarthy, C. 1999, ApJ, 512, L63
- White, R. D., Ghez, A. M., Reid, I. N., and Schultz, G. 1999, ApJ, 520, 811
- Wizinowich, P., Acton, D. S., Lai, O., Gathright, J., Lupton, W., and Stomski, P. 2000a, *Proceedings of the SPIE*, 4007, 2
- Wizinowich, P., Acton, D. S., Shelton, C., Stomski, P., Gathright, J., Ho, K., Lupton, W., Tsubota, K., Lai, O., Max, C., Brase, J., An, J., Avicola, K., Olivier, S., Gavel, D., Macintosh, B., Ghez, A., Larkin, J. 2000b, PASP, 112, 315

Zuckerman, B., and Becklin, E. E. 1993, *ApJ*, 406, L25

Fig. 1.— Narrow-band silicate filter images of HD 98800 taken with the OSCIR mid-IR camera. North is up and east is to the left. The broad-band filter images, K, M, N and IHW18, are not shown. The $0.''8$ binary is easily resolved; the airy ring appears as lobes around the northern component, HD 98800 B.

Fig. 2.— From left to right, respectively, the J, H, and K-band reconstructed speckle images of HD 98800. North is up and east is to the left; each frame is $\sim 1.3'' \times 1.3''$.

Fig. 3.— H-band images of HD 98800 without (left) and with (right) the Keck adaptive optics (AO) system. Without AO, the FWHM of the sources is $0.''4$. When AO is used, the FWHM drops to $0.''06$.

Fig. 4.— Azimuthally averaged profiles of HD 98800 A and B at four narrow-band wavelengths, 8.8, 9.8, 10.3 and $11.7\mu\text{m}$. The solid lines join the B component independent data points, and the dot-dash lines the A component independent points.

Fig. 5.— Azimuthally averaged AO H-band data for HD 98800 A and B and the point source SAO 180158. No significant differences are apparent in the three profiles. We use the lower and upper bounds in the errors for HD 98800 A and B, respectively, to determine an upper limit on the amount of reflected light from the dust in the H-band around HD 98800 B.

Fig. 6.— Spectral energy distributions for HD 98800 A, left, and HD 98800 B, right. For HD 98800 A, no excess emission is evident out to the longest observed wavelength of $18.2\mu\text{m}$; the 3932 K black body is plotted for reference. The 3562 K black body fit to HD 98800 B is also shown.

Fig. 7.— The subcomponents HD 98800 Aa, Ba, and Bb plotted on Baraffe et al. (1998) PMS evolutionary tracks. The 1.0 and 1.5 solar mass tracks are from models of Palla & Stahler (1999).

Fig. 8.— Masses of HD 98800 Ba (M_1) and Bb (M_2) as a function of orbital inclination of the Ba–Bb spectroscopic binary. The shaded areas correspond to 1σ range for the masses derived from the tracks of Baraffe et al. (1998) and the curved lines represent the 1σ range for the mass functions from Torres et al. (1995). The vertical solid lines delineate the range of allowed inclination given the constraints on the masses and mass functions.

Fig. 9.— The HD 98800 excess emission after subtraction of the stellar photosphere, represented by Kurucz model photometry. The data are fit extremely well by a 150 K black body, with the exception of the silicate emission feature at $10\mu\text{m}$. The 0.8, 1.1 and 1.3mm data are from Rucinski (1993), Sylvester et al. (1996), and Stern, Weintraub, and Festou (1993), respectively.

Table 1. Results of Disk Modelling

Wavelength (μm)	Dust/Photosphere Ratio	Radius 3σ Upper Limit (AU)
8.8	2.13	2.1
9.8	5.26	2.1
10.3	6.50	1.7
11.7	10.89	1.9

Table 2. HD 98800 Flux Densities

Instrument	Date	Filter	$\lambda(\mu m)$	$\Delta\lambda(\mu m)$	$F_\nu(total)$ (Jy)	B/A	$F_\nu(A)$ (Jy)	$F_\nu(B)$ (Jy)	Ref
WFPC2	1996 Mar 3	F439W	0.429	0.046	0.391±0.009	0.470±0.020	0.266±0.008	0.125±0.004	1
WFPC2	1996 Mar 3	F555W	0.525	0.122	1.129±0.025	0.615±0.026	0.699±0.021	0.430±0.013	1
WFPC2	1996 Mar 3	F953N	0.955	0.005	3.891±0.083	0.945±0.040	2.001±0.060	1.890±0.057	1
NICMOS	1998 May 1	F095N	0.954	0.009	3.958±0.084	0.904±0.004	2.076±0.062	1.882±0.056	2
NICMOS	1997 Jul 3	F108N	1.082	0.009	4.747±0.103	0.943±0.007	2.443±0.075	2.304±0.070	2
NICMOS	'97/'98	F145M	1.452	0.197	4.966±0.105	1.011±0.002	2.470±0.074	2.496±0.075	2
NCIMOS	1997 Jul 3	F187N	1.875	0.019	4.585±0.099	1.091±0.005	2.193±0.067	2.392±0.073	2
NICMOS	1998 May 1	F190N	1.899	0.017	4.705±0.100	1.045±0.003	2.301±0.069	2.404±0.072	2
NIRC	1996 Jan 6	J	1.251	0.292	4.25±0.09	1.096±0.110	2.03±0.15	2.22±0.15	3
NIRC	1996 Jan 5	H	1.658	0.333	4.79±0.10	1.067±0.107	2.32±0.17	2.47±0.17	3
NIRC ^a	1996 Jan 4	Kcont	2.210	0.04	3.58±0.11	1.002±0.100	1.79±0.14	1.79±0.14	3
KCAM+AO ^a	1999 May 25	H	1.648	0.317	4.79±0.10	0.991±0.075	2.41±0.14	2.38±0.14	3
OSCIR	1998 May 10	K	2.20	0.41	3.58±0.11	1.001±0.051	1.79±0.10	1.79±0.10	3
OSCIR	1998 May 10	M	4.80	0.60	1.03±0.05	1.282±0.141	0.45±0.05	0.58±0.06	3
OSCIR	1998 May 10	7.9	7.90	0.76	0.61±0.06	2.370±0.213	0.18±0.03	0.43±0.05	3
OSCIR	1998 May 10	8.8	8.80	0.87	1.09±0.06	4.505±0.183	0.20±0.02	0.89±0.05	3
OSCIR	1998 May 10	9.8	9.80	0.95	1.63±0.08	8.929±0.319	0.16±0.01	1.47±0.08	3
OSCIR	1998 May 10	10.3	10.30	1.01	1.75±0.09	11.905±0.425	0.14±0.01	1.61±0.09	3
OSCIR ^a	1998 May 10	N	10.80	5.23	1.506±0.151	12.821±0.657	0.109±0.016	1.397±0.145	3
OSCIR	1998 May 10	11.7	11.70	1.11	2.17±0.11	14.286±0.612	0.14±0.01	2.03±0.11	3
OSCIR	1998 May 10	12.5	12.50	1.16	2.34±0.12	16.129±1.561	0.14±0.02	2.20±0.12	3
OSCIR	1998 May 10	IHW18	18.2	1.65	5.004±0.500	58.824±13.841	0.084±0.028	4.920±0.511	3
TIMMI ^b	1996 Apr 5	M	4.71	0.99	0.90±0.17	1.00±0.15	0.45±0.09	0.45±0.09	4
TIMMI ^b	1996 Apr 5	N2	9.78	1.29	1.40±0.16	3.70±0.56	0.30±0.07	1.10±0.07	4
IRAS ^a	1983	12	12	7.5	2.36±0.14	—	—	2.36±0.14	2

Table 2—Continued

Instrument	Date	Filter	$\lambda(\mu m)$	$\Delta\lambda(\mu m)$	$F_\nu(total)$ (Jy)	B/A	$F_\nu(A)$ (Jy)	$F_\nu(B)$ (Jy)	Ref
IRAS	1983	25	25	11	9.74 ± 0.78	—	—	9.74 ± 0.78	2
IRAS	1983	60	60	40	7.05 ± 0.70	—	—	7.05 ± 0.70	2
IRAS	1983	100	100	37	4.31 ± 0.30	—	—	4.31 ± 0.30	2
JCMT ^a	1992 Feb	800	800	—	0.111 ± 0.012	—	—	0.111 ± 0.012	5
JCMT	1993 Apr 25	800	800	—	0.102 ± 0.010	—	—	0.102 ± 0.010	6
JCMT	1992 Feb,Mar	1100	1100	—	0.063 ± 0.006	—	—	0.063 ± 0.006	5
JCMT ^a	1994 Apr	1300	1300	—	0.011 ± 0.003	—	—	0.011 ± 0.003	5
IRAM	1993 Apr 17	1300	1300	—	0.036 ± 0.007	—	—	0.036 ± 0.007	7

^aData was not used in black body fits or plotted in figures.

^bData plotted in figures but not used in black body fits.

Note. — Values of $F_\nu(total)$ for NIRC, KCAM and most OSCIR data from ZB93; $F_\nu(total)$ for OSCIR N and IHW18 filters and all NIRC, KCAM and OSCIR flux ratios from this work.

References. — (1) Soderblom et al. 1998; K. Noll priv. comm.; (2) Low et al. 1999; (3) This work; (4) Gehrz et al. 1999; (5) Sylvester et al. 1996; (6) Rucinski 1993; (7) Stern et al. 1993

Table 3. HD 98800 Derived Stellar Parameters

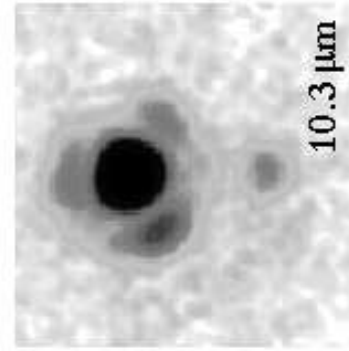
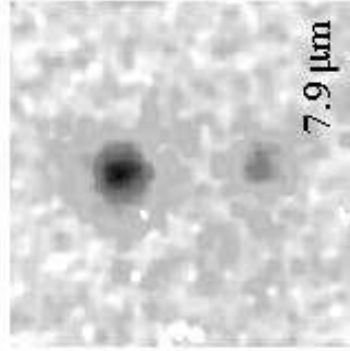
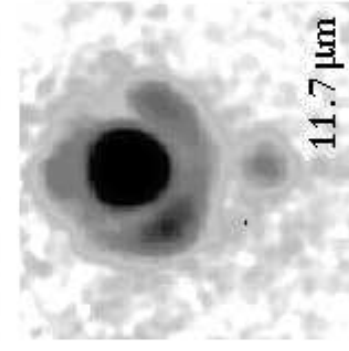
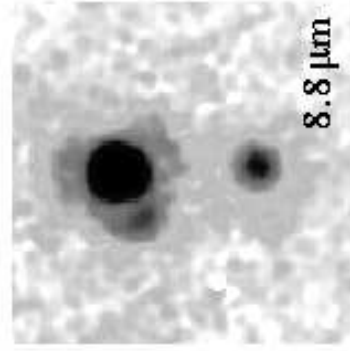
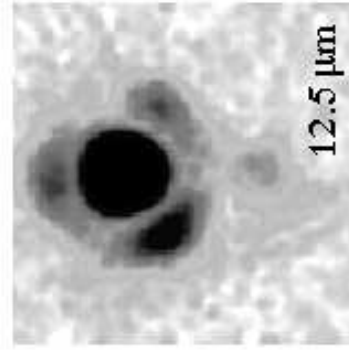
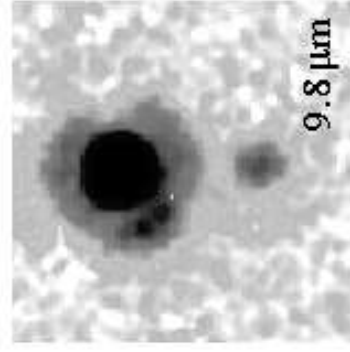
Component	T_{BB} (K)	T_{Kurucz} (K)	L_{BB} (L_{\odot})	L_{Kurucz} (L_{\odot})	R_{BB} (R_{\odot})	M (M_{\odot})
A (South)	3932 ± 5	4500 ± 250	0.63 ± 0.12	0.71 ± 0.14	1.71 ± 0.23	1.1 ± 0.1^a
B (North)	3562 ± 3	4000 ± 250	0.58 ± 0.11	0.58 ± 0.11	2.00 ± 0.27	1.6 ± 0.1^b

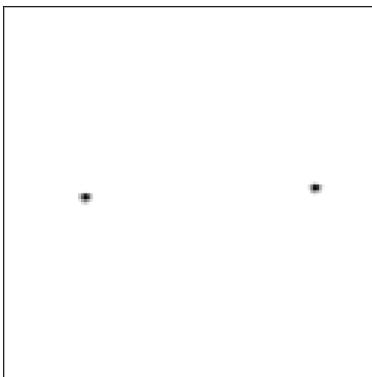
^aPrimary only.

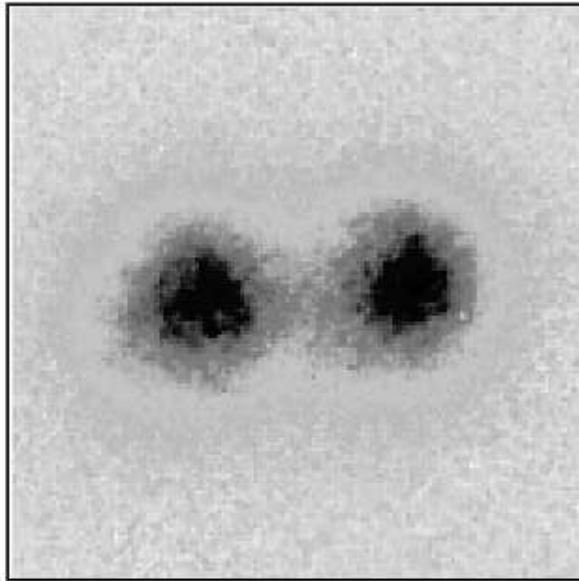
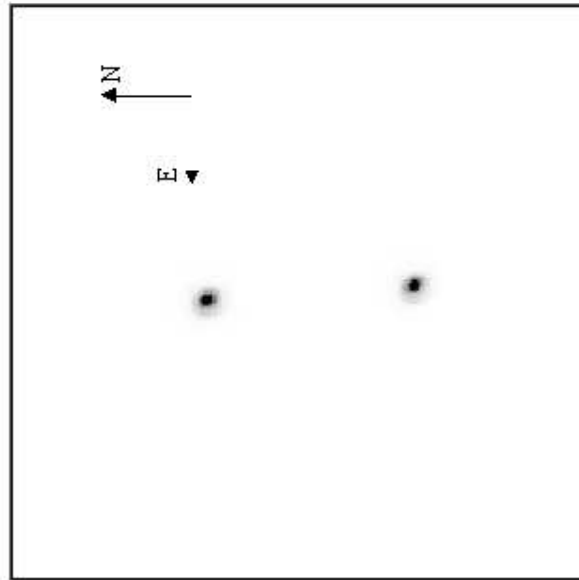
^b $M_{Ba} \sim 0.93$ and $M_{Bb} \sim 0.64 M_{\odot}$.

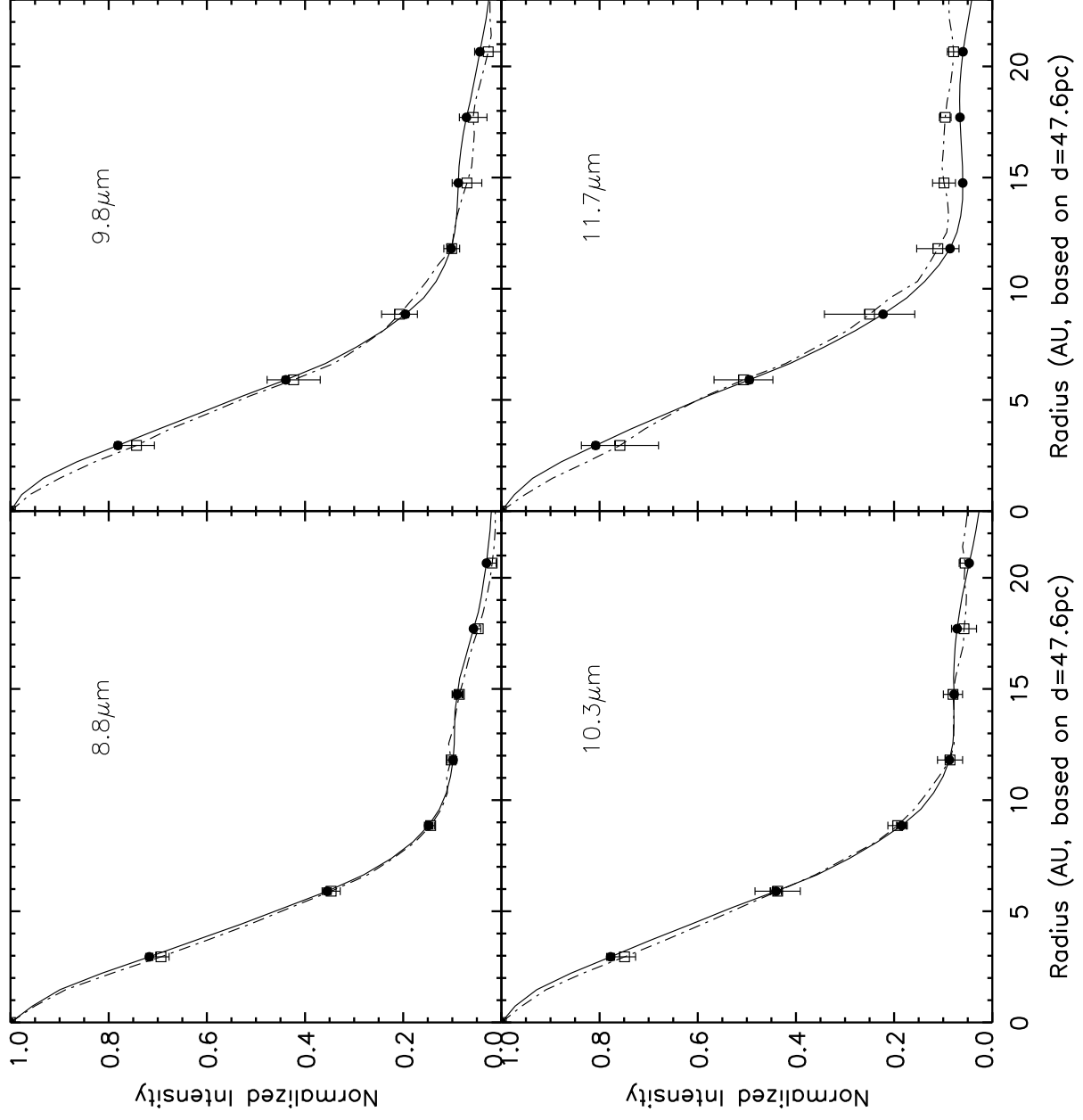
Table 4: HD 98800 Dust Parameters

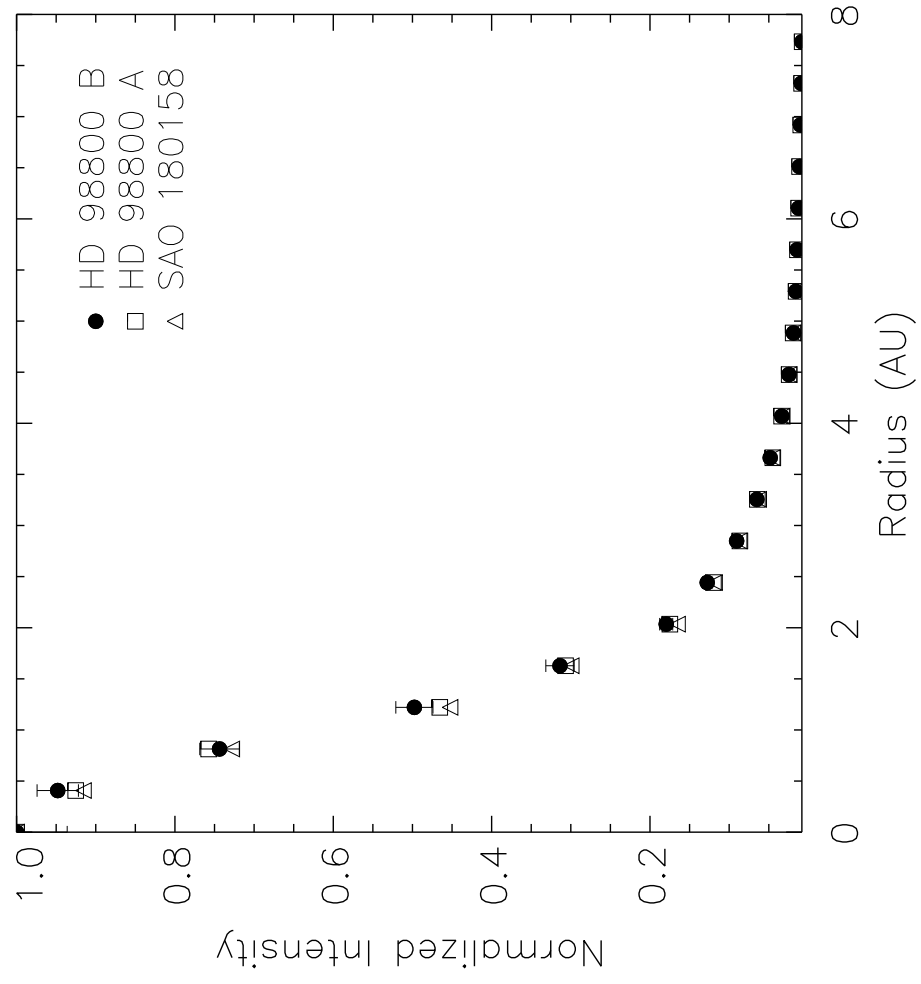
Blackbody Temperature	150 ± 5 K
Luminosity	$0.11 \pm 0.02 L_{\odot}$
Dust Grain Albedo	< 0.2
Dust Equilibrium Radius	2.4 ± 0.3 AU
Inner Disk Radius	1–2 AU
Outer Disk Radius	10–15 AU

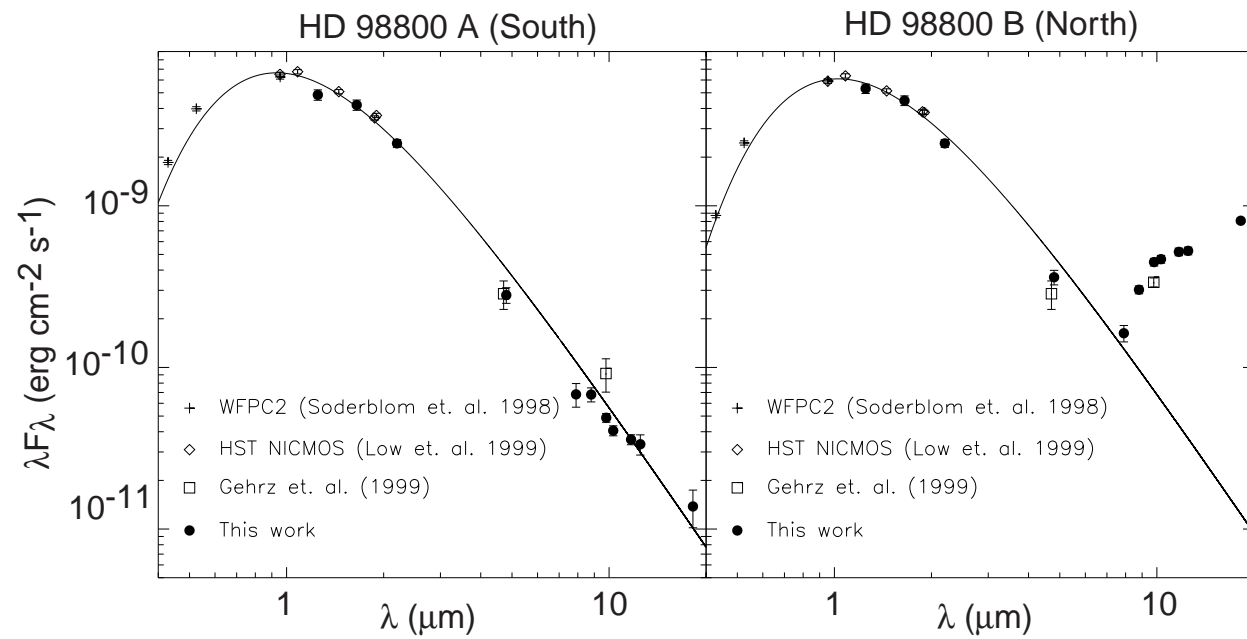


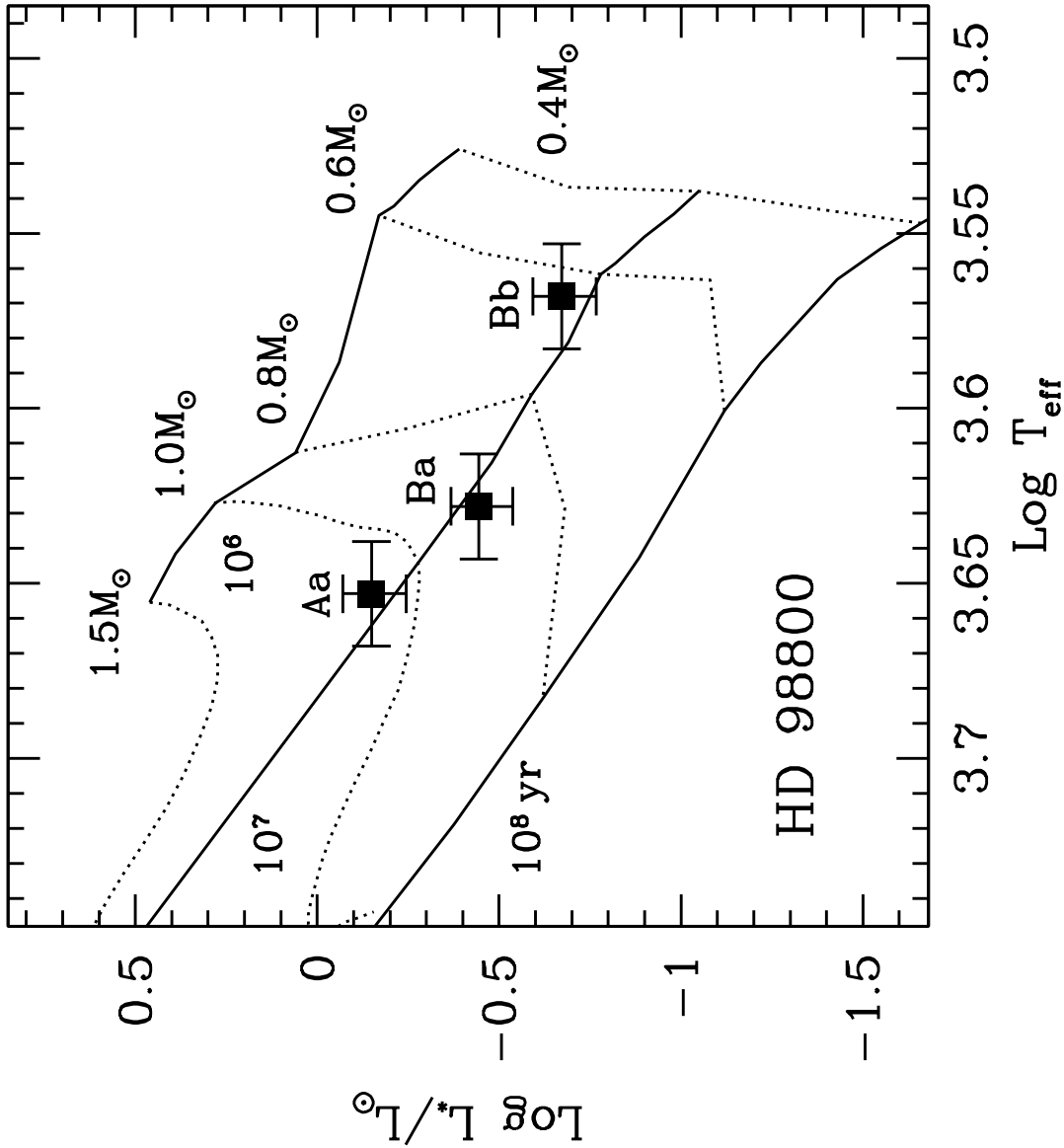


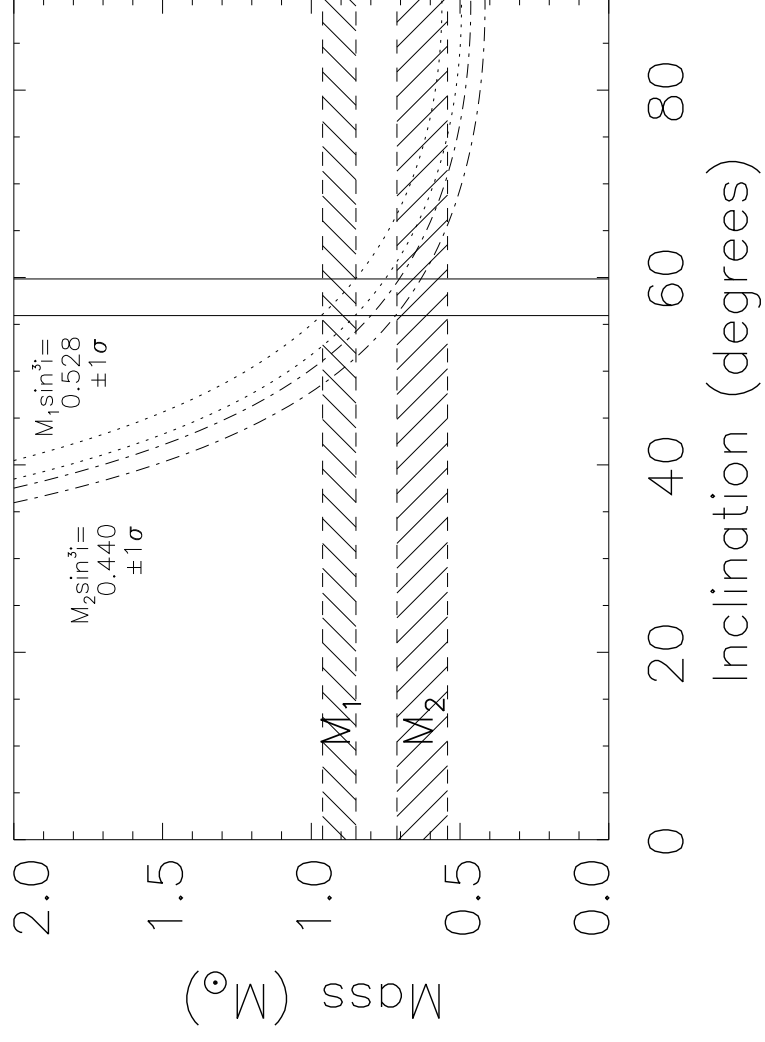












HD 98800 B: Dust Component Only

